Low-Complexity Detection for Space-Time Block Coded Spatial Modulation with Cyclic Structure

Babatunde S. Adejumobi and Narushan Pillay
School of Engineering, University of KwaZulu-Natal, Durban, 4041, South Africa
Email: adejumobibabatunde@gmail.com; pillayn@ukzn.ac.za

Abstract — This paper proposes a low-complexity near-maximum-likelihood (ML) detector for space-time block coded spatial modulation with cyclic structure (STBC-CSM). The proposed detector yields a significant reduction in computational complexity compared to the traditional ML detector, while simulation results demonstrate near-ML error performance. The union bound theoretical framework to quantify the average bit-error probability of M-ary quadrature amplitude modulation STBC-CSM over a frequency-flat Rayleigh fading channel is formulated and validates the Monte Carlo simulation results.

Index Terms—Low-complexity detection, Near-ML detection, Orthogonal projection, Space-time block coded spatial modulation, Space-time block coded spatial modulation with cyclic structure, Spatial modulation

I. Introduction

The demand for improved data services has become a necessity in modern day wireless communication [1, 2]. Space-time block coded (STBC) spatial modulation (STBC-SM) [3], a novel multiple-input multiple-output (MIMO) based transmission system, which exploits the advantages of both the Alamouti STBC and SM [4], have the potential to meet this demand. STBC-SM employs a pair of transmit antennas selected from a spatial (antenna) constellation to transmit a pair of amplitude and/or phase modulation (APM) constellation symbols over two time-slots [2, 3]. Since the transmit antenna pair indices and the APM symbols of STBC-SM are employed in transmitting information, the spectral efficiency (SE)/error performance is improved compared to Alamouti STBC and SM.

Several schemes, which make use of the STBC-SM technique, have been proposed. For example, labeling diversity was applied to STBC-SM in [5], similar to the method of [2, 6], to improve error performance. In [7], STBC-SM with cyclic structure (STBC-CSM), employs cyclic rotation of activated transmit antenna pairs within a codebook to transmit Alamouti codewords taken from two different constellation sets, thereby significantly increasing the SE of conventional STBC-SM. STBC-SM with temporal modulation (STBC-TSM) [8], was proposed to further improve the SE of STBC-SM, by employing a cyclic spatially rotated codebook with temporal permutations. However, although STBC-TSM is able to further improve the SE of STBC-SM, the computational complexity (CC) per time-slot, in terms of real multiplications, was 90% greater than STBC-CSM [8]. Hence, STBC-CSM is still of interest.

The advantages of STBC-CSM are reduced because of the CC imposed by the maximum-likelihood (ML) detector employed. The optimal ML detector for STBC-CSM in [7] has a large CC as it performs an exhaustive search over all possible matrices, thereby making it impracticable, especially when high-order M-ary APM constellations are employed. Although, linear detectors can be employed to reduce the CC due to the orthogonality of the STBC-CSM codeword [3, 7], this is only applicable in quasi-static fading channels.

In [9], orthogonal projection (OP) of signals was employed as a tool to reduce the CC of a MIMO system. Furthermore, in [5], OP was employed to reduce the CC of STBC-SM with labeling diversity, the results in both cases demonstrated near-ML error performance and a significant reduction in CC when compared with their corresponding ML detectors.

Furthermore, although simulated error performances of STBC-CSM were reported in [7], there was no theoretical framework to validate the average bit-error probability (ABEP).

Based on the above motivations, we propose a closed-form expression to evaluate the ABEP of STBC-CSM. Furthermore, we propose a LC detector based on OP of signals, which yields a near-ML error performance. In addition, we present an analytical framework to determine the CC of the proposed detector.

The remainder of this paper is organized as follows: Section II presents the background of STBC-CSM. The proposed theoretical framework of the union bound on the ABEP for STBC-CSM is then presented. The proposed near-ML LC detector of STBC-CSM is then formulated and the CC of the detectors are analyzed. In Section III, the numerical results are presented and discussed, and finally, the paper is concluded in Section IV.

Notation: The following notations are employed throughout this paper; bold and capital letters represent matrices, while bold small letters denote column vectors of matrices. $(\cdot)^{-1}$, $(\cdot)^{T}$, . $(\cdot)^{H}$ and $(\cdot)^{*}$ represents inverse, transpose, Hermitian and complex conjugate, respectively. $Q(\cdot)$ and $\|\cdot\|_F$ denotes Q-function and Frobenius norm, respectively. Also, $\operatorname{argmin}_w(\cdot)$ represents the minimum of an argument with respect to w

Manuscript received January 1, 2018; revised June 21, 2018.
Corresponding author email: adejumobibabatunde@gmail.com.
doi:10.12720/jcm.13.7.391-395

and $\lfloor w \rfloor_{2p}$ denotes the floor of the nearest power of two, less than or equal to w. $\boldsymbol{I}_w$ denotes a $w \times w$ identity matrix having all elements in its diagonal as unity.

II. STBC-CSM

A. Background/System Model

Given N_t transmit antennas, the STBC-CSM code set, which employs several transmit antenna pairs denoted as (t_1, t_2), where $t_1, t_2 \in [1\colon N_t]$ comprises of $N_t - 1$ codebooks, $\boldsymbol{\chi}_k$, $k \in [1\colon N_t - 1]$. Each codebook contains N_t codewords. The l-th, $l \in [1\colon N_t]$ codeword of the k-th codebook of STBC-CSM is given by $\boldsymbol{\chi}_{k,l} = \boldsymbol{G}^{l-1}\boldsymbol{D}_k e^{j\theta_k}$ [7], where θ_k is the optimized rotation angle of the k-th codebook given in (Table II, [7]), $\boldsymbol{G}$ is an $N_t \times N_t$ right-shift matrix [7] with $\boldsymbol{G}^0 = \boldsymbol{I}_{N_t}$ and $\boldsymbol{D}_k$ is an $N_t \times 2$ matrix defined as [7]:

$$\boldsymbol{D}_k = \begin{array}{c} \begin{bmatrix} x_p & 0 & \cdots & x_q & \cdots & 0 \\ -x_q^* & 0 & \cdots & x_p^* & \cdots & 0 \end{bmatrix}^T \\ \qquad\qquad (1+k)-th \quad column \end{array} \tag{1}$$

where x_p, $p \in [1\colon M]$ is a symbol from an M-ary quadrature amplitude modulation (M-QAM) constellation Ω_1, and x_q, $q \in [1\colon M]$ is a symbol from a rotated M-QAM constellation $\Omega_2 = \Omega_1 e^{j\phi}$, where ϕ is the optimized rotation angle of Ω_2 given in (Table II, [7]). The number of usable codewords is $c = \lfloor N_t(N_t-1) \rfloor_{2p}$ [7], yielding a SE of $0.5\log_2 c + \log_2 M$ bits/s/Hz. In the case of STBC-SM, $c = \left\lfloor \binom{N_t}{2} \right\rfloor_{2p}$.

Given the transmission of the codeword $\boldsymbol{\chi}_\ell = \boldsymbol{\chi}_{k,l}$, for the ℓ-th, $\ell \in [1\colon c]$ transmit antenna pair, where $\ell = N_t(k-1) + l$, the received STBC-CSM signal vectors for time-slots 1 and 2 may be formulated as [5]:

$$\boldsymbol{y}_1 = \sqrt{\frac{\rho}{2}}\left(\boldsymbol{h}^1_{\ell,t_1} s^1_p + \boldsymbol{h}^1_{\ell,t_2} s^1_q\right) + \boldsymbol{\eta}_1 \tag{2}$$

$$\boldsymbol{y}_2 = \sqrt{\frac{\rho}{2}}\left(\boldsymbol{h}^2_{\ell,t_1} s^2_q + \boldsymbol{h}^2_{\ell,t_2} s^2_p\right) + \boldsymbol{\eta}_2 \tag{3}$$

where $\boldsymbol{y}_i$, $i \in [1\colon 2]$ is an $N_r \times 1$ received signal vector for the i-th time-slot. $\frac{\rho}{2}$ is the average signal-to-noise ratio (SNR) at each receive antenna. $s^1_p = x_p e^{j\theta_k}$ and $s^1_q = x_q e^{j\theta_k}$ are the transmitted symbols for time-slot 1, while $s^2_q = -\left(x_q e^{j\theta_k}\right)^*$ and $s^2_p = \left(x_p e^{j\theta_k}\right)^*$ are transmitted in time-slot 2. $\boldsymbol{h}^i_{t_1}, \boldsymbol{h}^i_{t_2} \in \boldsymbol{H}_i$ are the channel vectors between the ℓ-th, $\ell \in [1\colon c]$ pair of transmit antennas (t_1, t_2) and the N_r receive antennas. $\boldsymbol{H}_i = \left[\boldsymbol{h}^i_{\ell,1} \quad \boldsymbol{h}^i_{\ell,2} \quad \cdots \quad \boldsymbol{h}^i_{\ell,N_t}\right]$, denotes the $N_r \times N_t$ Rayleigh frequency-flat fading channel, where the channel is assumed constant during each time-slot and takes on independent values in time-slot i [6]. $\boldsymbol{h}^i_{\ell,\varphi} = \left[\boldsymbol{h}^{i,\ell}_{\varphi,1} \quad \boldsymbol{h}^{i,\ell}_{\varphi,2} \quad \cdots \quad \boldsymbol{h}^{i,\ell}_{\varphi,N_r}\right]^T$, $\varphi \in [1\colon N_t]$ are $N_r \times 1$ column vectors of the φ-th transmit antenna. $\boldsymbol{\eta}_i$ denotes the $N_r \times 1$ additive white Gaussian noise (AWGN) vector. The entries of $\boldsymbol{H}_i$ and $\boldsymbol{\eta}_i$ are independent and identically distributed (i.i.d.) over time-slot i according to the $CN(0,1)$ distribution.

The optimal ML detector of STBC-CSM performs a joint detection to estimate the index of transmit antenna pair and the transmitted symbol and is defined as:

$$\begin{aligned}[\hat{\ell}, \hat{p}, \hat{q}] = \underset{\substack{\hat{x}_p \in \Omega_1, \hat{x}_q \in \Omega_2 \\ \hat{\ell} \in [1:c]}}{\operatorname{argmin}} \Bigg(\Bigg\| \boldsymbol{y}_1 & - \sqrt{\frac{\rho}{2}}\left(\boldsymbol{h}^1_{\ell,t_1} s^1_p + \boldsymbol{h}^1_{\ell,t_2} s^1_q\right)\Bigg\|_F^2 \\ & + \Bigg\| \boldsymbol{y}_2 - \sqrt{\frac{\rho}{2}}\left(\boldsymbol{h}^2_{\ell,t_1} s^2_q + \boldsymbol{h}^2_{\ell,t_2} s^2_p\right)\Bigg\|_F^2 \Bigg)\end{aligned} \tag{4}$$

where $\hat{\ell}$, $\hat{p}$ and $\hat{q}$ denote the estimates of ℓ, p and q, respectively.

The ML detector imposes a high CC as will be discussed in Section II.C, hence the need for a LC detector.

B. Proposed ABEP Analysis for STBC-CSM

Employing a union bound, the ABEP may be formulated as:

$$ABEP \leq \frac{1}{cM^2} \sum_{\boldsymbol{S}} \sum_{\widehat{\boldsymbol{S}}} \frac{N_{\boldsymbol{S}\widehat{\boldsymbol{S}}} P\left(\boldsymbol{S} \to \widehat{\boldsymbol{S}}\right)}{\log_2 c + 2\log_2 M} \tag{5}$$

where $P\left(\boldsymbol{S} \to \widehat{\boldsymbol{S}}\right)$ is the pairwise error probability (PEP) given that the transmitted codeword $\boldsymbol{S}$ is received as $\widehat{\boldsymbol{S}}$. $N_{\boldsymbol{S}\widehat{\boldsymbol{S}}}$ is the number of bits in error that is associated with the PEP event $P\left(\boldsymbol{S} \to \widehat{\boldsymbol{S}}\right)$. $\boldsymbol{S}$ is an $N_t \times 2$ transmit codeword having s^i_p, $i \in [1\colon 2]$ and s^i_q as the only non-zero elements in the i-th column corresponding to the t_1-th and t_2-th positions, respectively. $\widehat{\boldsymbol{S}}$ is an erroneous received version of $\boldsymbol{S}$.

Consider $\boldsymbol{H}_1 = \left[\boldsymbol{h}^1_{\ell,t_1} \quad \boldsymbol{h}^1_{\ell,t_2}\right]$ and $\boldsymbol{H}_2 = \left[\boldsymbol{h}^2_{\ell,t_1} \quad \boldsymbol{h}^2_{\ell,t_2}\right]$, $\boldsymbol{H}_1, \boldsymbol{H}_2 \in \boldsymbol{H}$, the conditional PEP $P\left(\boldsymbol{S} \to \widehat{\boldsymbol{S}} | \boldsymbol{H}\right)$ may be formulated as [2]:

$$\begin{aligned}P\left(\boldsymbol{S} \to \widehat{\boldsymbol{S}} | \boldsymbol{H}\right) = P \Bigg(\Bigg\| \boldsymbol{y}_1 & - \sqrt{\frac{\rho}{2}}\left(\boldsymbol{h}^1_{\hat{\ell},t_1} s^1_{\hat{p}} + \boldsymbol{h}^1_{\hat{\ell},t_2} s^1_{\hat{q}}\right)\Bigg\|_F^2 \\ & + \Bigg\| \boldsymbol{y}_2 - \sqrt{\frac{\rho}{2}}\left(\boldsymbol{h}^2_{\hat{\ell},t_1} s^2_{\hat{q}} + \boldsymbol{h}^2_{\hat{\ell},t_2} s^2_{\hat{p}}\right)\Bigg\|_F^2 \\ & < \|\boldsymbol{\eta}_1\|_F^2 + \|\boldsymbol{\eta}_2\|_F^2 \Bigg)\end{aligned} \tag{6}$$

Similar to the method of [6], (6) can be simplified as [2, 6]:

$$\begin{aligned}& P\left(\boldsymbol{S} \to \widehat{\boldsymbol{S}} | \boldsymbol{H}\right) \\ & = Q\left(\sqrt{\frac{\rho}{8} \|\boldsymbol{H}_1\|_F^2 \|\boldsymbol{S}_1\|_F^2 + \|\boldsymbol{H}_2\|_F^2 \|\boldsymbol{S}_2\|_F^2}\right)\end{aligned} \tag{7}$$

where $\boldsymbol{S}_1 = \widehat{\boldsymbol{S}}_{c_1} - \boldsymbol{S}_{c_1}$ and $\boldsymbol{S}_2 = \widehat{\boldsymbol{S}}_{c_2} - \boldsymbol{S}_{c_2}$, $\widehat{\boldsymbol{S}}_{c_i}$ and $\boldsymbol{S}_{c_i}$, $i \in [1:2]$ denotes the i-th column of $\widehat{\boldsymbol{S}}$ and $\boldsymbol{S}$, respectively. Similar to [6], based on the moment generating function (MGF), the unconditional PEP $P(\boldsymbol{S} \to \widehat{\boldsymbol{S}})$ is defined as [2, 6]:

$$P(\boldsymbol{S} \to \widehat{\boldsymbol{S}}) = \frac{1}{2g}\left[\frac{1}{2}M_1\left(\frac{1}{2}\right)M_2\left(\frac{1}{2}\right) + \sum_{v=1}^{g-1} M_1\left(\frac{1}{2\sin^2\theta_v}\right)M_2\left(\frac{1}{2\sin^2\theta_v}\right)\right] \tag{8}$$

where $M_1(w) = \left(\frac{1}{1+2w\sigma_{\alpha_i}^2}\right)^{N_r}$, $i \in [1:2]$, $\sigma_{\alpha_i}^2 = \frac{\rho}{8}\|\boldsymbol{S}_i\|_F^2$ and $\theta_v = \frac{v\pi}{2g}$ with g the number of iterations needed for convergence of the trapezoidal approximation of the Q-function.

C. Proposed LC Detector for STBC-CSM

In this section, motivated to reduce the CC of STBC-CSM, we propose a near-ML LC detector based on OP [5] to reduce the CC of the STBC-CSM ML detector.

A LC detector for STBC-CSM, which employs OP, firstly selects ξ_1 and ξ_2 likely candidates $\boldsymbol{z}_p^\ell = [\hat{z}_{p,1}^\ell \quad \hat{z}_{p,2}^\ell \quad \cdots \quad \hat{z}_{p,\xi_1}^\ell]$ and $\boldsymbol{z}_q^\ell = [\hat{z}_{q,1}^\ell \quad \hat{z}_{q,2}^\ell \quad \cdots \quad \hat{z}_{q,\xi_2}^\ell]$ of the transmitted symbols s_p^1 and s_q^1, respectively, for the ℓ-th transmit antenna pair, where $\ell \in [1:c]$, $\boldsymbol{z}_p^\ell \subseteq \Omega_1 e^{j\theta_k}$ and $\boldsymbol{z}_q^\ell \subseteq \Omega_2 e^{j\theta_k}$, with $\xi_1\xi_2 \ll M^2$.

Employing the method in [5, 9], the projection matrix $\boldsymbol{P}_{\ell,t_a}^i$, where $i, a \in [1:2]$, which corresponds to the projection space $\boldsymbol{h}_{\ell,t_a}^i$ is computed, such that $\boldsymbol{P}_{\ell,t_a}^i \boldsymbol{h}_{\ell,t_a}^i = 0$. The projection matrix $\boldsymbol{P}_{\ell,t_a}^i$ may be defined as [5]:

$$\boldsymbol{P}_{\ell,t_a}^i = \boldsymbol{I}_{N_r} - \boldsymbol{h}_{\ell,t_a}^i\left(\left(\boldsymbol{h}_{\ell,t_a}^i\right)^H \boldsymbol{h}_{\ell,t_a}^i\right)^{-1}\left(\boldsymbol{h}_{\ell,t_a}^i\right)^H \tag{9}$$

where $\boldsymbol{P}_{\ell,t}$ projects a signal orthogonal to the subspace of the channel vector $\boldsymbol{h}_{\ell,t_a}^i$. $\boldsymbol{h}_{\ell,t_a}^i$ is the channel vector of the t_a-th transmit antenna during the i-th time-slot. If $\hat{z}_{p,m}^\ell = s_p^1$, $m \in [1:\xi_1]$ and $\hat{z}_{q,n}^\ell = s_q^1$, $n \in [1:\xi_2]$, then the sum of the projections can be formulated as [5]:

$$\boldsymbol{P}_{\ell,t_2}^1\left(\boldsymbol{y}_1 - \sqrt{\frac{\rho}{2}}\boldsymbol{h}_{\ell,t_1}^1 \hat{z}_{p,m}^\ell\right) + \boldsymbol{P}_{\ell,t_1}^2\left(\boldsymbol{y}_2 - \sqrt{\frac{\rho}{2}}\boldsymbol{h}_{\ell,t_2}^2\left(\hat{z}_{p,m}^\ell\right)^*\right) = \boldsymbol{P}_{\ell,t_2}^1\boldsymbol{\eta}_1 + \boldsymbol{P}_{\ell,t_1}^2\boldsymbol{\eta}_2 = \psi_1 \tag{10}$$

$$\boldsymbol{P}_{\ell,t_1}^1\left(\boldsymbol{y}_1 - \sqrt{\frac{\rho}{2}}\boldsymbol{h}_{\ell,t_2}^1 \hat{z}_{q,n}^\ell\right) + \boldsymbol{P}_{\ell,t_2}^2\left(\boldsymbol{y}_2 + \sqrt{\frac{\rho}{2}}\boldsymbol{h}_{\ell,t_1}^2\left(\hat{z}_{q,n}^\ell\right)^*\right) = \boldsymbol{P}_{\ell,t_1}^1\boldsymbol{\eta}_1 + \boldsymbol{P}_{\ell,t_2}^2\boldsymbol{\eta}_2 = \psi_2 \tag{11}$$

however, if $\hat{z}_{p,m}^\ell \neq s_p^1$ and $\hat{z}_{q,n}^\ell \neq s_q^1$, the sum of the projections in (10) and (11) yields [5]:

$$\boldsymbol{P}_{\ell,t_2}^1\left(\sqrt{\frac{\rho}{2}}\boldsymbol{h}_{\ell,t_1}^1\left(s_p^1 - \hat{z}_{p,m}^\ell\right)\right) + \boldsymbol{P}_{\ell,t_1}^2\left(\sqrt{\frac{\rho}{2}}\boldsymbol{h}_{\ell,t_2}^2\left(s_p^2 - \left(\hat{z}_{p,m}^\ell\right)^*\right)\right) + \psi_1 \tag{12}$$

$$\boldsymbol{P}_{\ell,t_1}^1\left(\sqrt{\frac{\rho}{2}}\boldsymbol{h}_{\ell,t_2}^1\left(s_q^1 - \hat{z}_{q,n}^\ell\right)\right) + \boldsymbol{P}_{\ell,t_2}^2\left(\sqrt{\frac{\rho}{2}}\boldsymbol{h}_{\ell,t_1}^2\left(s_q^2 + \left(\hat{z}_{q,n}^\ell\right)^*\right)\right) + \psi_2 \tag{13}$$

From [5], it can be deduced that the Frobenius norms of (12) and (13) are greater than the Frobenius norms of (10) and (11), respectively. Hence, based on OP, the proposed LC near-ML detection algorithm for the STBC-CSM system follows:

Step 1: Compute the projection spaces $\boldsymbol{r}_{\ell,t_a,s_p}^i$ and $\boldsymbol{r}_{\ell,t_a,s_q}^i$, $i, a \in [1:2]$, $p, q = [1:M]$, $\ell = [1:c]$ given in (14)-(17), and the projection matrices $\boldsymbol{P}_{\ell,t_a}^i$ formed from (9) for the ℓ-th antenna pair [5].

$$\boldsymbol{r}_{\ell,t_1,s_p}^1 = \boldsymbol{y}_1 - \sqrt{\frac{\rho}{2}}\boldsymbol{h}_{\ell,t_1}^1 s_p^1 \tag{14}$$

$$\boldsymbol{r}_{\ell,t_2,s_q}^1 = \boldsymbol{y}_1 - \sqrt{\frac{\rho}{2}}\boldsymbol{h}_{\ell,t_2}^1 s_q^1 \tag{15}$$

$$\boldsymbol{r}_{\ell,t_1,s_q}^2 = \boldsymbol{y}_2 - \sqrt{\frac{\rho}{2}}\boldsymbol{h}_{\ell,t_1}^2 s_q^2 \tag{16}$$

$$\boldsymbol{r}_{\ell,t_2,s_p}^2 = \boldsymbol{y}_2 - \sqrt{\frac{\rho}{2}}\boldsymbol{h}_{\ell,t_2}^2 s_p^2 \tag{17}$$

Step 2: Determine ξ_1 and ξ_2 most likely candidate sets $\boldsymbol{z}_p^\ell = [\hat{z}_{p,1}^\ell \quad \hat{z}_{p,2}^\ell \quad \cdots \quad \hat{z}_{p,\xi_1}^\ell]$ and $\boldsymbol{z}_q^\ell = [\hat{z}_{q,1}^\ell \quad \hat{z}_{q,2}^\ell \quad \cdots \quad \hat{z}_{q,\xi_2}^\ell]$, respectively, for the ℓ-th transmit antenna pair by choosing ξ_1 and ξ_2 symbols, which gives the smallest projection norms from the metrics given in (18) and (19), respectively.

$$\hat{z}_p^{\ell} = \underset{r_{\ell,t_a,sp}^{i}}{\operatorname{argmin}} \left\| \boldsymbol{P}_{\ell,t_2}^{1} \boldsymbol{r}_{\ell,t_1,s_p}^{1} + \boldsymbol{P}_{\ell,t_1}^{2} \boldsymbol{r}_{\ell,t_2,s_p}^{2} \right\|_F^2 \tag{18}$$

$$\hat{z}_q^{\ell} = \underset{r_{\ell,t_a,sq}^{i}}{\operatorname{argmin}} \left\| \boldsymbol{P}_{\ell,t_1}^{1} \boldsymbol{r}_{\ell,t_2,s_q}^{1} + \boldsymbol{P}_{\ell,t_2}^{2} \boldsymbol{r}_{\ell,t_1,s_q}^{2} \right\|_F^2 \tag{19}$$

where $p, q \in [1\!:\!M]$.

Step 3: Determine $\hat{\ell}$, $\hat{p}$ and $\hat{q}$ by an exhaustive search across all elements in $\boldsymbol{z}_p^{\ell}$ and $\boldsymbol{z}_q^{\ell}$ for all antenna pairs by employing the ML rule according to [5]:

$$\begin{aligned}[\hat{\ell}, \hat{p}, \hat{q}] = \underset{\hat{\ell}\in[1:c], \boldsymbol{z}_p^{\ell}, \boldsymbol{z}_q^{\ell}}{\operatorname{argmin}} \Bigg(& \left\| \boldsymbol{y}_1 - \sqrt{\frac{\rho}{2}} \left(\boldsymbol{h}_{\ell,t_1}^{1} \hat{z}_{p,m}^{\ell} + \boldsymbol{h}_{\ell,t_2}^{1} \hat{z}_{q,n}^{\ell} \right) \right\|_F^2 \\ & + \Bigg\| \boldsymbol{y}_2 \\ & - \sqrt{\frac{\rho}{2}} \Big(\boldsymbol{h}_{\ell,t_2}^{2} \left(\hat{z}_{p,m}^{\ell} \right)^* \\ & - \boldsymbol{h}_{\ell,t_1}^{2} \left(\hat{z}_{q,n}^{\ell} \right)^* \Big) \Bigg\|_F^2 \Bigg) \end{aligned} \tag{20}$$

where $\hat{z}_{p,m}^{\ell} \in \boldsymbol{z}_p^{\ell}$, $\hat{z}_{q,n}^{\ell} \in \boldsymbol{z}_q^{\ell}$, $\ell \in [1\!:\!c]$, $m \in [1\!:\!\xi_1]$ and $n \in [1\!:\!\xi_2]$.

D. CC Analysis

Similar to [1, 5], the CC in terms of complex operations are formulated. Furthermore, we assume that calculated values are stored in memory, hence, redundant operations are not considered.

Computing $\boldsymbol{h}_{\ell,t_1}^{1} s_p^1$, $\boldsymbol{h}_{\ell,t_2}^{1} s_q^1$, $\boldsymbol{h}_{\ell,t_1}^{2} s_q^2$ and $\boldsymbol{h}_{\ell,t_2}^{2} s_p^2$ in (4) requires $4N_r$ complex multiplications. Also, another $4N_r$ complex additions are required to sum elements within the Frobenius norm operators. Since there are two Frobenius norm operators having operations of an $N_r \times 1$ vector, an additional $2N_r$ complex multiplications and $2N_r - 2$ complex additions are added to the CC. Furthermore, because an exhaustive search, which involves c iterations of the complex operations mentioned is to be performed, the total CC in terms of complex operations of the ML detector becomes:

$$\delta_{ML} = cM^2(12N_r - 2) \tag{21}$$

For the LC detection algorithm, the CC involved in computing the four projection matrices $\boldsymbol{P}_{\ell,t_1}^{1}$, $\boldsymbol{P}_{\ell,t_2}^{1}$, $\boldsymbol{P}_{\ell,t_1}^{2}$ and $\boldsymbol{P}_{\ell,t_2}^{2}$ in (18) and (19) is given as [5]:

$$\delta_{pm} = c(8N_r^2 + 12N_r - 4) \tag{22}$$

To determine the ξ_1 and ξ_2 estimates of x_p and x_q most likely candidates give n in (18) and (19), the CC is given as [5]:

$$\delta_{lc} = c(8MN_r^2 + 16MN_r - 4N_r + 4M) \tag{23}$$

The solution for the CC of the exhaustive ML search in (20), across the most likely candidates $\boldsymbol{z}_p^{\ell}$ and $\boldsymbol{z}_q^{\ell}$ is similar to the ML search in (4), however, the CC is reduced because the search is across $\xi_1\xi_2$ symbols, and $\xi_1\xi_2 \ll M^2$. Hence, the total CC for this stage is given as:

$$\delta_{ML_{lc}} = c\xi_1\xi_2(12N_r - 2) \tag{24}$$

The total CC in terms of complex operations of the proposed LC near-ML detector may be defined as:

$$\begin{aligned}\delta_{STBC-CSM\ LC} = \delta_{pm} + \delta_{lc} + \delta_{ML_{lc}} \\ = 2c[4N_r^2(M+1) \\ + 2N_r(4M + 3\xi_1\xi_2 + 4) \\ - (2M + \xi_1\xi_2 + 2)]\end{aligned} \tag{25}$$

Table I presents numerical values of the CCs in terms of complex operations for the ML and LC detectors, with SE = 5 and 6 bits/s/Hz. The LC detector yields a 59% and 66% reduction in CC over the ML detector for SE = 5 and 6 bits/s/Hz, respectively.

TABLE I: COMPARISON OF CCS BETWEEN ML AND LC DETECTORS

STBC-CSM CONFIGURATION	SE	ML	LC
$N_t = 3$, $N_r = 4$, $c = 4$, $M = 16$, $\xi_1 = 6$, $\xi_2 = 6$	5	47,104	19,408
$N_t = 5$, $N_r = 4$, $c = 4$, $M = 16$, $\xi_1 = 6$, $\xi_2 = 3$	6	188,416	64,384

III. NUMERICAL RESULTS

In this section, the bit-error rate (BER) of STBC-CSM with 16-QAM and $N_r = 4$ is demonstrated for the ML detector and the proposed LC detector. The formulated theoretical ABEP is also evaluated and used to validate the ML detection simulation results.

In Fig. 1 and Fig. 2, the notation (N_t, N_r, c, M, SE) is employed to denote the configuration of STBC-CSM

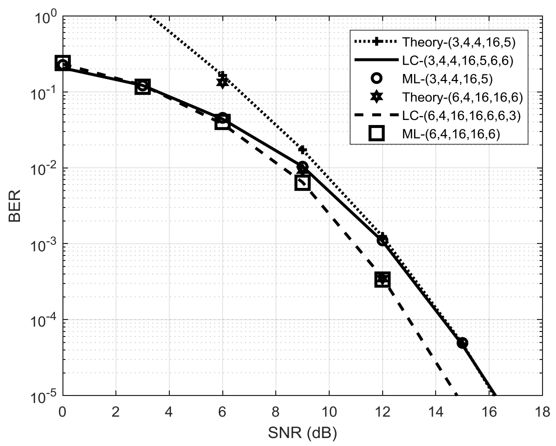

Fig. 1. BER performances for ML, LC detectors including theoretical ABEP of the STBC-CSM ML detector employing; $N_t = 3$, $c = 4$, SE = 5 bits/s/Hz and $N_t = 6$, $c = 16$, SE = 6 bits/s/Hz.

when the ML detector is employed, while (N_t, N_r, c, M, SE, ξ_1, ξ_2) is employed to denote the configuration of STBC-CSM when the LC detector is employed.

In all simulations, the BER of the LC detector demonstrates a close match with the ML detector as depicted in Fig. 1 and Fig. 2. It is also evident that the evaluated theoretical ABEP agrees well with the ML detection simulation results at high SNRs.

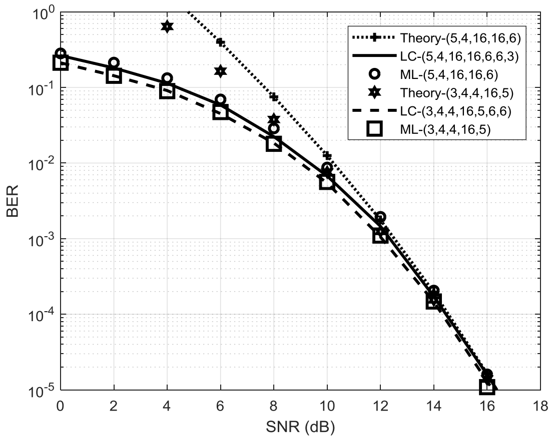

Fig. 2. BER performances for ML, LC detectors including theoretical ABEP of the STBC-CSM ML detector employing; $N_t = 3$, $c = 4$, SE = 5 bits/s/Hz and $N_t = 6$, $c = 16$, SE = 6 bits/s/Hz.

IV. CONCLUSION

The theoretical ABEP of STBC-CSM with M-QAM was formulated and validates simulation results at high SNR. Furthermore, a LC near-ML detector based on OP was formulated and matches very closely with the ML detector, while significantly reducing CC.

REFERENCES

[1] B. S. Adejumobi, N. Pillay, and S. H. Mneney, "A study of spatial media-based modulation using RF mirrors," in *Proc. IEEE AFRICON*, Sep. 2017, pp. 336–341.

[2] N. Pillay and H. Xu, "Uncoded space-time labeling diversity - application of media-based modulation with RF mirrors," *IEEE Commun. Lett.*, 2017.

[3] E. Basar, U. Aygolu, E. Panayirci, and H. V. Poor, "Space-time block coded spatial modulation," *IEEE Trans. Commun.*, vol. 59, no. 3, pp. 823–832, Mar. 2011.

[4] D. Lee, S. Nooshabadi, and K. Kim, "Dual-mode SM/STBC system with antenna subset selection employing ML detection," *AEU-Int. J. Electron. Commun.*, vol. 64, no. 12, pp. 1128–1136, Dec. 2010.

[5] K. Govindasamy, H. Xu, and N. Pillay, "Space-time block coded spatial modulation with labeling diversity," *Int. J. Commun. Syst.*, 2017.

[6] H. Xu, K. Govindasamy, and N. Pillay, "Uncoded space-time labeling diversity," *IEEE Commun. Lett.*, vol. 20, no. 8, pp. 1511–1514, Aug. 2016.

[7] X. Li and L. Wang, "High rate space-time block coded spatial modulation with cyclic structure," *IEEE Commun. Lett.*, vol. 18, no. 4, pp. 532–535, Apr. 2014.

[8] A. G. Helmy, M. D. Renzo, and N. Al-Dhahir, "Enhanced-reliability cyclic generalized spatial-and-temporal modulation," *IEEE Commun. Lett.*, vol. 20, no. 12, pp. 2374–2377, Dec. 2016.

[9] S. Bahng, S. Shin, and Y. O. Park, "ML approaching MIMO detection based on orthogonal projection," *IEEE Commun. Lett.*, vol. 11, no. 6, pp. 474–476, Jun. 2007.

Babatunde Segun Adejumobi received B.Sc. and M.Sc. degree in Electronic and Computer Engineering from the Lagos State University, Lagos, Nigeria. He is currently pursuing a Ph.D. degree with the Department of Electrical, Electronic and Computer Engineering University of KwaZulu-Natal, Durban, South Africa. His current research includes spatial modulation, space-time block coded modulation and orthogonal frequency division multiplexing. However, he also has interest in optical communication, wireless communications and Image processing.

Dr. Narushan Pillay received the MSc.Eng (cum laude) and PhD degree in wireless communications from the University of KwaZulu-Natal, South Africa, Durban, in 2008 and 2012, respectively. He has been with the University of KwaZulu-Natal since 2009. Previously, he was with the Council of Scientific and Industrial Research (CSIR) in South Africa. His research interests are in physical wireless communications, including spectrum sensing for cognitive radio and MIMO systems. He has published several papers in well-known journals in his area of research. Dr Pillay currently supervises several PhD and MSc.Eng students.